Impact of the intermediate principal stress on rock strength: Polyaxial testing and numerical simulations.

Helle Foged Christensen
GEO, Maglebjergvej 1, DK-2800 Lyngby, Denmark, e-mail hfc@geoteknisk.dk

Nils Kågeson Loe
BP EPTG, Chertsey Road, Sunbury-on-Thames Middlesex TW16 7LN

Bertold Plischke
ISAMGEO Engineering GmbH, Junkernstr. 35, D-65205 Wiesbaden, Germany

Ole Havmøller
Norsk Hydro, PB 7190, N-5020 Bergen, Norway

Morten Gjetting Stage
GEO, Maglebjergvej 1, DK-2800 Lyngby, Denmark

ABSTRACT:

Most conventional rock mechanics tests have their origin in civil engineering, where design rules necessarily dictate a conservative approach. For the petroleum industry applications however, partial rock failure may be acceptable in order to optimize design. If such approaches are to be adopted in a manner other than purely empirically then the method of stability analysis must fully account for the failure behaviour of intact rock; i.e. the transition from peak to residual strength including the change in friction, dilatancy and cohesion characteristics and not least, the role of the intermediate principal stress. A number of polyaxial tests have been carried out on Saltwash North and Castlegate outcrop sandstone, and compared to results from conventional triaxial tests. The test results have been back analyzed using the ISAMGEO FE code. The results of the study confirm that the intermediate principal stress does have an impact on rock failure and that this is not adequately captured by the standard Mohr-Coulomb criterion. In response a modified Mohr-Coulomb criterion is established. Furthermore, using a simple example of openhole stability, the study demonstrates that the results of numerical modeling are sensitive to the method adopted during model calibration in addition to accounting for the intermediate principal stress and post-peak strength strain softening. These effects will have a critical impact on engineering design if this is to include partial rock failure.

1. INTRODUCTION

Most conventional rock mechanics tests have their origin in civil engineering where design rules necessarily must be conservative. As such, both tests and geotechnical design have primarily focused on pre-failure behaviour where the rock is largely intact and elastic, and the determination of the peak strength. In contrast, for some oil reservoir applications partial rock failure may be acceptable in order to optimize design. Under some drilling applications partial failure of the wellbore wall (breakout development) may be acceptable or even desirable in order to reduce mud weight provided there is adequate hole cleaning. Alternatively in the design of multilateral well junctions significant cost reductions can be achieved if the junctions are completed without cemented casings [1]. Under these circumstances, a viable stability analysis must properly account for the post-peak strength behaviour, dilatancy and the effect of the intermediate principal stress. To meet this challenge, new and more advanced laboratory tests are required to provide the necessary information and numerical models must become more refined.

A number of polyaxial tests have been carried out on Saltwash North and Castlegate outcrop sandstone, and compared to results from conventional triaxial and uniaxial rock mechanic tests. The polyaxial test parameters were determined through pre-test numerical modeling where the intention was to design stress paths that simulated near-wellbore stress conditions. Subsequently the results from both the conventional and polyaxial tests were used in numerical analysis for the purposes of evaluating model refinement and constitutive model formulations where particular emphasis was placed on matching peak strength and post-peak stress-strain behaviour.

2. LABORATORY TESTING

A set of conventional and polyaxial rock mechanic tests were performed on the two outcrop sands used in the study, Castlegate and Saltwash North. Both sandstones are relatively homogenous, but where the Saltwash North has an unconfined compressive strength (UCS) of 16.5 MPa, the Castlegate sandstone is weaker with an UCS 5.7 MPa.

Table 1. Summary of types of rock mechanic tests performed in the study

	Test type
A	Unconfined Compression test, UCS
B	Triaxial tests (conventional)
C	Multiple failure triaxial tests
D	Polyaxial test

The UCS and conventional triaxial tests were performed in accordance with standard ISRM test procedures on cylindrical core plugs.

The polyaxial tests were carried out in GEO's custom made true 3D cell which allows the 3 principal stresses to be independently controlled. The cell consists of a steel body with 4 movable and flexible rubber cushions supplying the 2 lateral principal stresses. The vertical principal stress is established through moveable steel end pistons. The cell design allows for the control of pore pressure, and pore fluids including injection in horizontal and vertical directions. The rock specimens are box shaped with heights between 78 and 110 mm and with a cross-sectional area of approximately 46 x 46 mm.

The polyaxial test series was designed to study the near wellbore stress and strain states particularly how they evolve post drilling, as the well is drawndown. The near well bore environment can be treated as a plane strain problem, which eases numerical simulation. Two of the principal stresses are predefined (radial & tangential stress) whereas the third principal stress (axial stress, parallel to the wellbore axis) is variable and is determined by the rock's response to the imposed boundary condition of zero lateral strain. Assuming the third, independent, principal stress is the intermediate principal stress, the experiments can be used to study how this stress influences and is influenced by rock behaviour (e.g. peak strength) as well as test the ability of various constitutive models to correctly describe the effects observed.

The multiple failure triaxial tests were performed in accordance with international testing standards with the exception that they were performed in the 3D cell. This was purposely done as it made it possible to observe the difference between conventional and true-3D triaxial (polyaxial) tests.

2.1. Saltwash North sandstone strength

Figure 1 illustrates the peak and residual strength data obtained from the conventional triaxial tests and the polyaxial tests.

Referring to figure 1 it can be seen that the peak strength and residual strength values obtained from conventional triaxial tests are well described by the standard Mohr-Coulomb failure criterion (Figure 1). The relative reduction, from peak to residual, in friction angle (line gradient) and cohesion (y-axis intercept) clearly indicate the development of a shear plane once sample failure occurs, which is confirmed by the inspection of samples after testing.

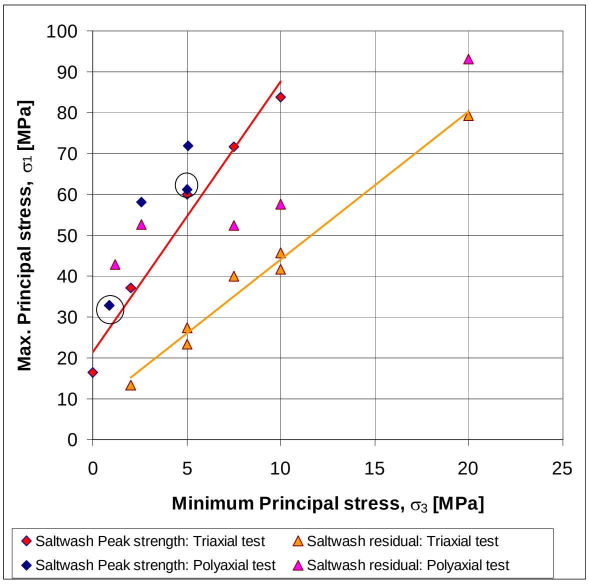

Fig. 1 Saltwash North Sandstone: Peak & Residual strength data measured from conventional triaxial tests, multiple failure triaxial tests & polyaxial tests. Circled polyaxial data points indicate stress paths where $\sigma_2 \approx \sigma_3$ (Lode angle ≈ 30°).

The peak strength measured from polyaxial tests where the lateral stresses are equal or nearly equal, $\sigma_2 \approx \sigma_3$, (including the first cycle of loading in the multiple failure triaxial test performed in the true 3D cell) are circled in the above plot. These data points coincide with the other peak strength data from the conventional triaxial tests. This is as expected given $\sigma_2 \approx \sigma_3$ in the tests.

The results from the polyaxial tests, where $\sigma_2 \neq \sigma_3$, are observed not to coincide with the Mohr-Coulomb failure criterion defined by the conventional triaxial tests. The magnitude of the stress anisotropy cannot be seen on a plot in figure 1, and an alternative plotting method is required in order to quantify the deficiency of the standard Mohr-Coulomb criterion. Figure 2 is a so-called Pi-plane plot: the Pi-plane is a projection of the yield surface (failure criterion) in principal stress space, normal to the hydrostatic axis ($\sigma_1 = \sigma_2 = \sigma_3$). The Mohr-Coulomb criterion appears as a hexagonal yield surface when viewed in the Pi-plane (figure 2).

The Pi-plane plot clearly demonstrates that the Mohr-Coulomb criterion under predicts peak rock strength, as measured in the polyaxial tests, for anisotropic stress states ($\sigma_1 > \sigma_2 > \sigma_3$). This mismatch suggests that an alternative failure criterion that adequately captures the influence of the intermediate stress, σ_2, is required.

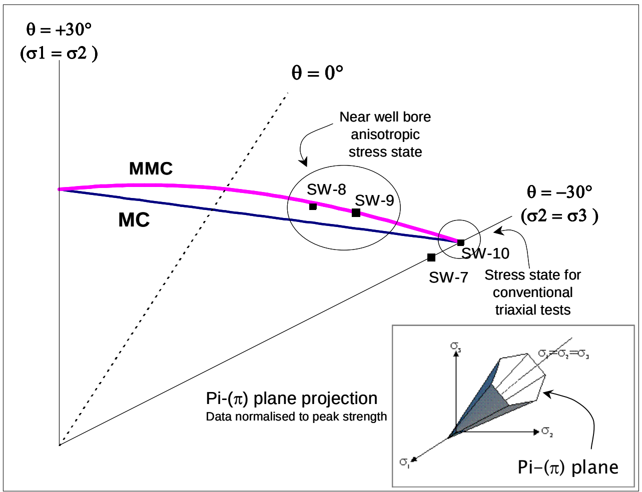

Fig 2. Pi (π)-plane projection showing peak strength measured in polyaxial (true triaxial) tests performed on *Saltwash North Sandstone*. Note: the data is normalized to peak strength thus enabling all the tests to be viewed collectively with respect to the failure criteria: MC – standard Mohr-Coulomb; MMC – Modified Mohr-Coulomb. *Inset* shows a 3-D projection of the Mohr-Coulomb yield surface in principal stress space. The Pi-plane is the projection (slice) of the yield surface perpendicular to the hydrostatic ($\sigma_1 = \sigma_2 = \sigma_3$) axis

2.2. Castlegate sandstone strength

Figure 3 illustrates the peak and residual strength data obtained from the conventional triaxial tests and the polyaxial tests performed on Castlegate sandstone.

From figure 3 it can be clearly seen that the standard Mohr-Coulomb criterion gives a satisfactory fit to the peak and residual strength data as measured in standard triaxial tests. As with the Saltwash North data the development of a shear plane during failure is indicated by the relative reduction in friction angle and cohesion values from peak to residual strength.

The peak strength measured from polyaxial tests where the lateral stresses are equal or nearly equal, $\sigma_2 \approx \sigma_3$, are circled in figure 3. Similarly to the Saltwash North data, this data point coincides with the other peak strength data from the conventional tests as is expected since $\sigma_2 = \sigma_3$ in the test.

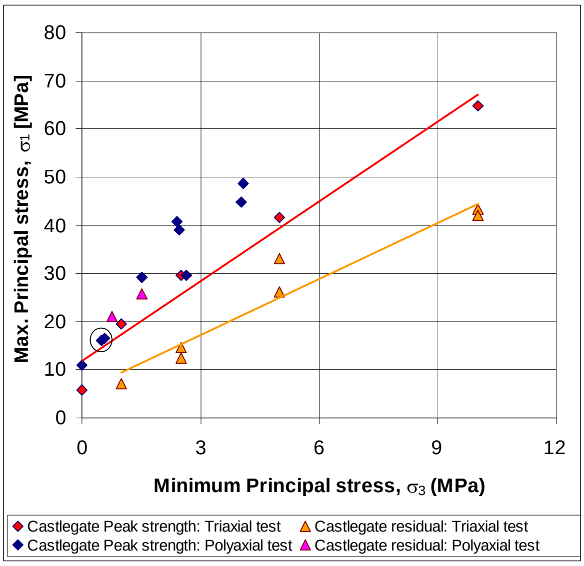

Fig. 3 Castlegate Sandstone: Peak & Residual strength data measured from conventional triaxial tests, multiple failure triaxial tests & polyaxial tests. . Circled polyaxial data points indicate stress paths where $\sigma_2 \approx \sigma_3$ (Lode angle $\approx 30^{o}$).

The results from the polyaxial tests do not coincide with the test results from the conventional triaxial tests (figure 3). This is in line with the observations on the Saltwash North sandstone and is attributed to the fact that the Mohr-Coulomb criterion under predicts peak rock strength for anisotropic stress states, i.e. $\sigma_2 > \sigma_3$. Figure 4, the Pi-plane plot, further emphasizes this observation.

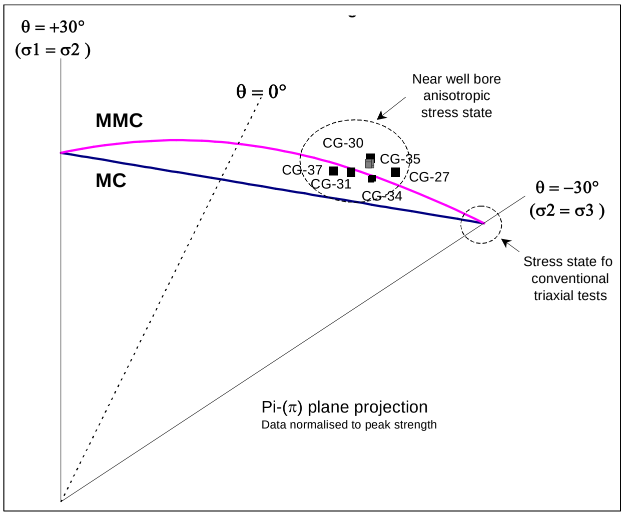

Fig 4. Pi (π)-plane projection showing peak strength measured in polyaxial (true triaxial) tests performed on *Castlegate Sandstone*. Note: the data is normalized to peak strength thus enabling all the tests to be viewed collectively with respect to the failure criteria: MC – standard Mohr-Coulomb; MMC – Modified Mohr-Coulomb.

3. MODELLING THE IMPACT OF THE INTERMEDIATE PRINCIPLE STRESS

The laboratory data for Saltwash North and Castlegate sandstone clearly indicate that for anisotropic stress conditions, particularly those representing the near well bore stress state, the standard Mohr-Coulomb criterion under predicts the peak rock strength. This effect has been observed by a number of other authors [2-9] and is nicely summarized by [2]. It is also the reason why there exists a number of different failure criteria (yield functions) which endeavor to capture the role of the intermediate stress on rock behaviour; e.g. Drucker-Prage, Lade-Ewy, William-Warnke.

In the course of this work a number of yield criteria were implemented in the ISAMGEO finite element code and tested for the purposes of back analyzing the laboratory data. Ultimately, a novel modification of the Mohr-Coulomb criterion was considered as especially suitable. This Modified Mohr-Coulomb (MMC) criterion extends the common Mohr-Coulomb criterion:

$$F = \sigma_1 \cdot (1 - \sin\varphi) - \sigma_3 \cdot (1 + \sin\varphi) - 2c\cos\varphi \quad \ldots(1)$$

by incorporating an additional term, which accounts for the intermediate principal stress:

$$F = \sigma_1 \cdot (1 - \sin\varphi) - \sigma_3 \cdot (1 + \sin\varphi) - 2c\cos\varphi - \frac{2\varsigma \cdot (\sigma_1 - \sigma_2) \cdot (\sigma_2 - \sigma_3)}{\sqrt{J_2}} \quad \ldots(2)$$

where:

J_2 is the second invariant of deviatoric stress and ζ is an additional material parameter.

The advantages of a Mohr-Coulomb based criterion is that it is 1) a well known model within geotechnical community, 2) the relatively few parameters are easily defined from standard laboratory experiments (apart from ζ), 3) the concept of non-associated flow can be easily implemented by exchanging friction with dilatancy angle in the necessary constitutive equations, 4) the model is readily implemented in a numerical code. The yield surface for the Modified Mohr-Coulomb and it's goodness-to-fit with respect to the laboratory data is shown in figures 2 & 4. Here it is seen that the modified criterion gives a near perfect description of how the intermediate principal stress, σ_2, influences peak rock strength. For Saltwash North, the fit is achieved by choosing $\zeta = 0.08$, for Castlegate sandstone, $\zeta = 0.10$ is used.

4. APPLYING THE MODIFIED MOHR-COULOMB CRITERION IN POST-FAILURE ANALYSIS

It was mentioned in the introduction that under certain circumstances allowing for partial rock failure in some drilling or completion applications might be acceptable or even desirable with respect to design optimization or cost benefit. To properly meet this challenge the numerical models used in the design analysis must be equipped to deal realistically with anisotropic stress states as well as post-peak strength stress-strain behaviour. This is a step out from conventional civil engineering, which generally bases design criteria on peak or residual strength - the transition from peak to residual strength is not considered. The simulation of this transition requires refined numerical techniques, as conventional finite element analyses based on classical continuum theories run into numerical problems, as the underlying differential equations are mathematically ill posed. This difficulty is overcome by means of a theory for frictional materials based on the Cosserat theory [10, 11]. It is a continuum model that also considers rotations of grains by introducing an additional degree of freedom. Such a Cosserat model is implemented in the applied finite element code. Thus it is possible to model the process of shear localization: after shear failure, strains are not homogeneously distributed but are localized in shear bands. A realistic post-peak stress-strain model should correctly relate the local stresses and strains, which is not reflected in the stress-strain curves recorded in laboratory tests relating average stresses and average strain. The full benefit of the above presented refined yield criterion, which incorporates the impact of the intermediate stress on rock failure behaviour is only gained, if the numerical model allows for a realistic description of the rock behaviour in the transition zone from peak strength to residual strength. The following provides an illustration.

4.1. Back-analysis of a polyaxial test

The process of numerical model calibration is illustrated through the back analysis of a Castlegate sandstone polyaxial test (CG-27). The test used emulates a plane strain condition whereby two of the principal stresses are predefined and the third varies in response to the imposed boundary condition of zero lateral strain. It is intended that the test represent conditions close to the borehole wall but it is also an ideal candidate for model calibration as the plane strain boundary conditions simplifies the numerical analysis.

The polyaxial test is back analyzed using 1) the conventional single element technique: i.e. where a single element represents the rock sample and stresses and strains are imposed at the cell boundary; and, 2) a finite element grid which represents both the sample and the loading platens (number of elements in the grid is 3060). The two approaches are used in order to see if differences in the method of calibration influence the results of forward modeling, e.g. open hole stability – see next section.

A single element model will not allow for strain localization where this can impact on the parameter values describing strain softening. The conventional use of single element models for back analysis overlooks the fact that deformation is focused along a discrete failure plane and that the remainder of the sample largely behaves as rigid body. The effect is to artificially smear the local strains over the whole element representing the rock sample (figure 5). Moreover, by adjusting the constitutive model until it matches the observed strain softening behaviour indirectly captures the process of strain localization. Thus the calibrated model can vary from the more refined approach using a finite element grid and Cosserat theory, for example, whereby strain localization is a product of the simulation.

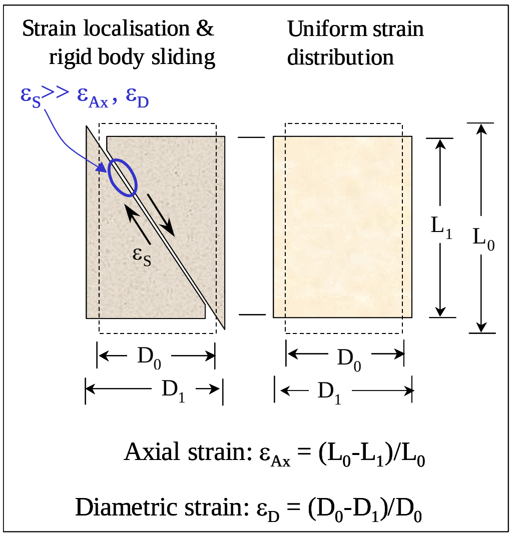

Figure 5 Illustration of strain distribution in a deformed rock sample: Strain localization & rigid body sliding (left) and homogenous (uniform) strain distribution (right). Single element numerical models assume the latter even though the former governs strain-softening behaviour. Refer to text for further discussion.

When using a finite element mesh and Cosserat theory to simulate test behaviour a number of additional parameters have to be considered. First, in Cosserat theory, an internal length parameter has to be defined and the value of this is generally unknown – in the cases presented here the internal length is set at 0.5 mm. Secondly, the steel loading platens should be included in the model mesh as correctly capturing the load distribution within the platen will influence the results – this is particularly important when modeling strain localization. As such it is also important to describe the load platen – sample interface. For the case presented here the interface elements are assumed to behave elastically but have reduced shear stiffness relative to the steel platen.

In the ISAMGEO code, the post-peak strength softening behaviour is determined by a set of decay laws describing the change in cohesion, friction and dilatancy angles (equations 3 & 4 respectively) and cohesion.

$$\varphi = \varphi_{res} + (\varphi_{peak} - \varphi_{res}) \cdot \exp(-\chi \cdot (\varepsilon_{pl} - \varepsilon_{pl}^{\ peak})) \quad ..(3)$$

The equation for describing the decay in dilatancy angle has a similar form to equation 3

$$c = c_0 - T \cdot (\varepsilon_{pl} - \varepsilon_{pl}^{\ peak}) \quad \ldots\ldots\ldots\ldots\ldots\ldots\ldots\ldots\ldots..(4)$$

In the above, T and χ are calibration constants and are determined by the back analysis of the laboratory test.

Referring to figures 6 to 8 and the stress-strain state during the polyaxial test. In the test the minimum principal stress, σ_3, is kept at 4 MPa while the axial stress (maximum principal stress) is increased until failure occurs. Once peak strength is reached the minimum stress is increased to reduce the rate of softening. The intermediate principal stress varies during the test as a function of the rock sample's deformation moduli and the imposed boundary condition of zero lateral strain.

The results from the numerical analysis using a single element are in good agreement with the laboratory data. The variation in the intermediate and minimum principal stresses are not shown for the finite element simulation as these stresses are not constant over the length of the sample. For the maximum principal stress (axial stress) – axial strain response, the finite element approach emulates the laboratory data more closely than the single element model in terms of pre- and post-failure stiffness. Both approaches show excellent match with the measured peak strength.

Figure 9 shows an output from the finite element simulation of the laboratory test in terms of equivalent plastic strain concentration. The conjugate shear planes are self-evident - the hot colours indicate a high strain concentration within the shear bands. Bearing in mind the earlier comments on strain "smearing" related to the single element approach to back analysis, it is worth noting that predicted strains within the shear zones exceed 20% but the measured global strains did not exceed 3% (figure 8).

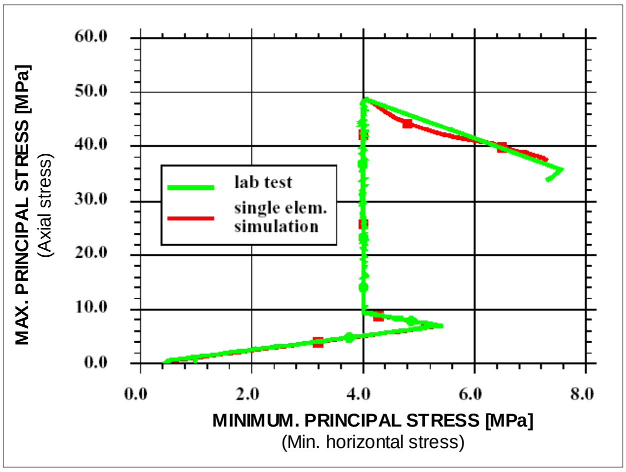

Figure 6 Stress path (σ_1 - σ_3) used in the polyaxial test CG-27 Plot shows values measured from test (green line) and values from numerical back-analysis (red line) - refer to text.

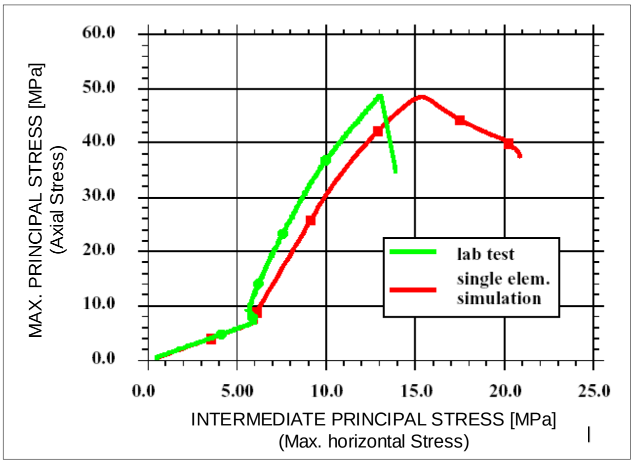

Figure 7. Stress path (σ_1 - σ_2) from the polyaxial test CG-27. The intermediate stress varies during the test as a function of the rock sample's stiffness and imposed boundary condition of zero lateral strain. Plot shows values measured from test (green) and values from numerical back-analysis (red).

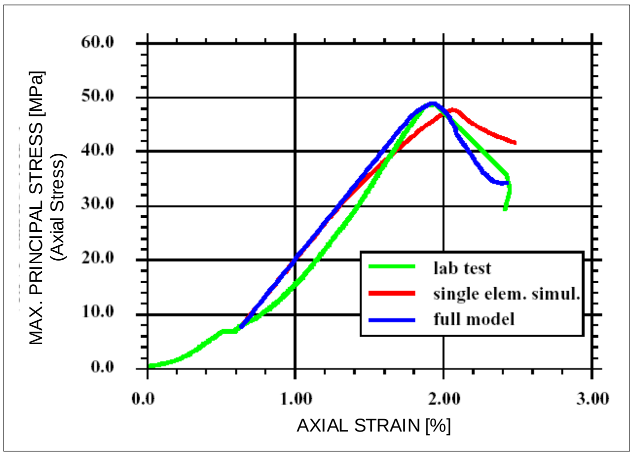

Figure 8. Axial stress-axial strain plot from the polyaxial test CG-27. Plot shows values measured from test (green line) and values from numerical back-analysis (blue & red lines) – refer to text.

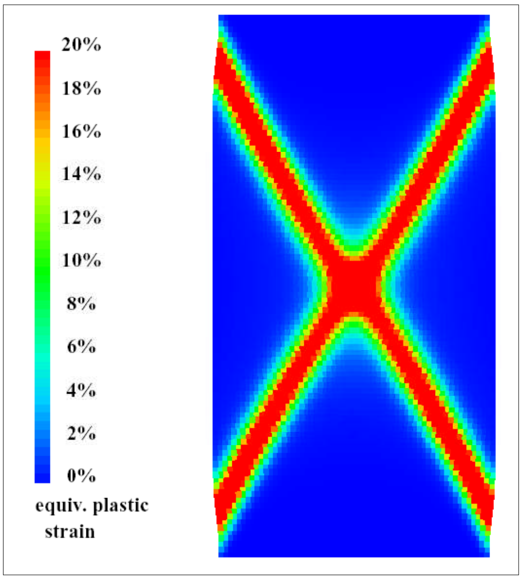

Figure 9. Output from numerical back analysis of polyaxial test, CG-27, showing the localization of plastic strain and the formation of conjugate shear plane pair.

Figure 10 is a sketch of the failure planes observed in the polyaxial test sample after it was removed from the apparatus. Relative to figure 9 only one shear plane is observed – no conjugate pair has developed. A probable cause is the presence of one or other imperfection in the rock sample that favours the growth of one shear plane over the other. The numerical simulation assumes no imperfections but from other studies it is known that the inclusion of imperfections can determine whether a single shear plane or a conjugate pair develop. Also the thickness of the shear plane in the post-test sample is much less than what was predicted from numerical analysis. This discrepancy is greater than to be expected from the inherent smoothening in the applied post processing software and is the subject of further investigation.

To further emphasize the difference in the two numerical approaches, table 2 summarizes the calibration parameters obtained from the back analysis of the polyaxial test.

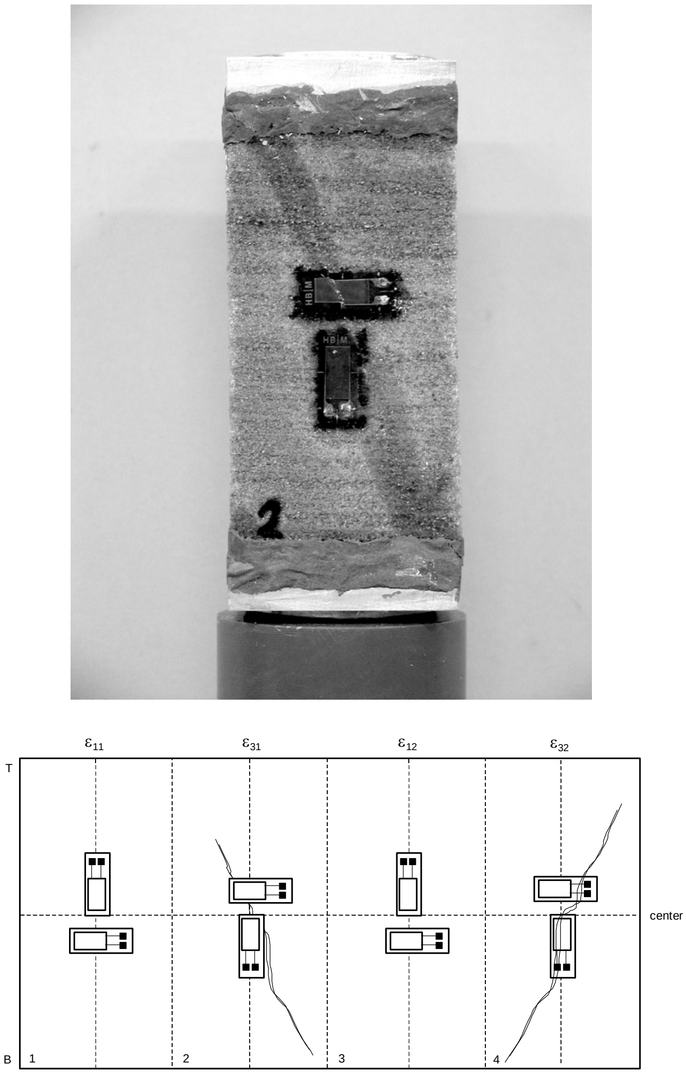

Figure 10. Photograph and sketch of polyaxial test sample, CG-27, after it has been removed from the test cell showing the location of fractures and shear planes. Note: The sketch is an unfolded view showing all 4 sides of the sample

Table 2 Calibration parameters from analysis of polyaxial test.

	Single element calibration	FE-grid calibration
Young's modulus E	3250 MPa	3250 MPa
Poisson's ratio ν	0.18	0.18
Angle of friction (peak/residual)	43.5° / 37°	43.5° / 37°
Dilatancy (peak/residual)	10° / 0°	35° / 30°
Cohesion (peak/residual)	3.6 / 0.01 MPa	3.6 / 0.01 MPa
equival. plastic strain at peak	0.5%	0.5%
parameter ζ for σ_2-impact	0.10	0.10
Cohesion softening parameter T	110 MPa	15 MPa
Coefficient χ for friction softening	30	10
Internal length parameter (Cosserat theory)	n/a	0.5 mm

4.2. Forward modeling – open hole stability

To illustrate how numerical model refinement can impact on design a relatively simple open hole stability problem is used. The objective of the exercise is to determine the stability of an horizontal open borehole located in a reservoir sandstone as the pore pressure is depleted (reduced) from 0 to 150 Bar (15 MPa). For consistency, in the model the reservoir is represented by Castlegate sandstone. The pre-depletion in-situ stress state at the depth of the borehole is given in table 3. In the exercise, the results of 3 different analyses are compared:

i. Standard Mohr-Coulomb criterion (no σ_2 impact) with strain softening, model calibration using single element approach (figures 11 & 12)

ii. Modified Mohr-Coulomb criterion (σ_2 impact) with strain softening, model calibration using single element approach (figures 11 & 13)

iii. Modified Mohr-Coulomb criterion (σ_2 impact) with strain softening, model calibration using finite element approach (figure 14)

Table 3 – Summary of in-situ stress state used in analysis

Eff. Vertical Stress [MPa] σ'_V	Eff. Horiz. Stress [MPa] ⊥ to well axis σ'_H	Eff. Horiz. Stress [MPa] || to well axis σ'_h	Reservoir Pressure [MPa] P_P
21	14	12	15

From figures 11 to 14 it is relatively obvious that a more refined approach to numerical analysis predicts a significantly smaller failure zone in the borehole wall. This is in part supported by field experience of applying standard Mohr-Coulomb criterion to borehole stability analysis for both drilling and production applications. Here experience indicates that the criterion is overly conservative – in its simplest form (ignoring strain softening) the standard Mohr-Coulomb criterion over-predicts the size of breakouts that may develop during drilling or predict the formation of breakouts where none are seen on caliper and image logs. Similarly sand prediction models using standard Mohr-Coulomb criterion conservatively predict sand production; i.e. model predicts sanding at an early stage than what is actually observed. In many cases these deficiencies are circumvented by either using work arounds, e.g. acceptable breakout angles, or by adjusting one or several input parameters, e.g. rock strength, pore pressure, in-situ stress.

Thus the impact on engineering due to the conservatism of the less refined models can be significant. In drilling it can affect the calculated safe mud weight or more importantly influence the casing design. In production it can determine whether or not an open hole completion is viable with respect to sanding risk and ultimately completion design [1].

5. CONCLUSION

The premise of this study has been to seek out a step change in the approach to borehole stability analysis by establishing a method that realistically accounts for partial rock failure. That is to say the transition from peak to residual strength including the change in friction, dilatancy and cohesion characteristics. In addition is also necessary to properly establish the role of the intermediate principal stress on rock behaviour as the type of yield criterion employed in the analysis will have a significant impact on the final results.

The results from polyaxial and conventional triaxial tests performed as part of this study confirm that the intermediate principal stress does have an impact on rock failure and that this is not adequately captured by the standard Mohr-Coulomb criterion. The test results were back-analyzed using the ISAMGEO FE code with special emphasis on correctly modeling the effect of the intermediate principal stress, post-peak strength strain softening and strain localization. This allowed a modified Mohr-Coulomb criterion to be established.

Furthermore, using a simple example of open hole stability, the study demonstrates that the results of numerical modeling are sensitive to the method adopted during model calibration in addition to accounting for the intermediate principal stress and post-peak strength strain softening. These effects will have a critical impact on engineering design if this is to include partial rock failure.

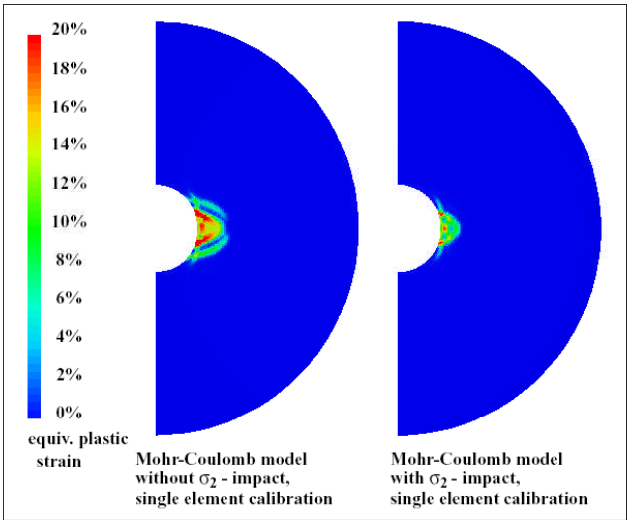

Figure 11 Openhole stability simulation using *standard Mohr-Coulomb* criterion (no σ_2 impact), *left*, and *Modified Mohr-Coulomb* (with σ_2 impact), *right*. Results show plastic strain magnitude & localization around the hole wall post-drilling (Drawdown = 0 Bar; i.e. well in balance).

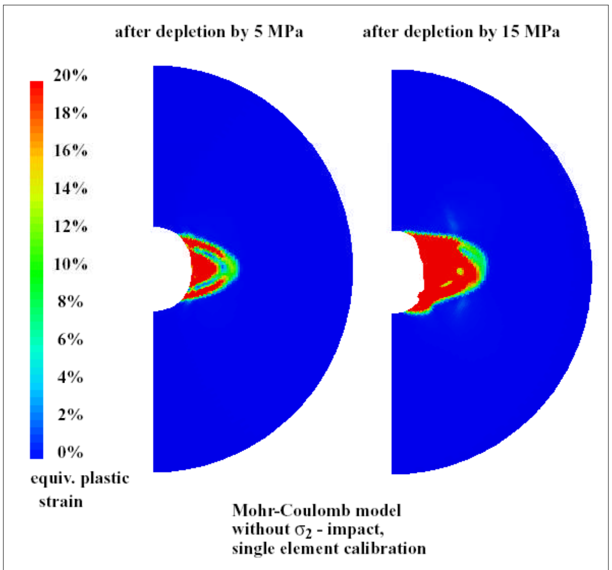

Figure 12 Openhole stability simulation using standard Mohr-Coulomb criterion (no σ_2 impact). The numerical model is calibrated using a *single element* back-analysis of a polyaxial test. Results show plastic strain magnitude & localization around the hole wall with increasing depletion: 5 MPa (50 Bar), *left* & 15 MPa (150 Bar) *right*.. Results can be compared with figures 13 & 14.

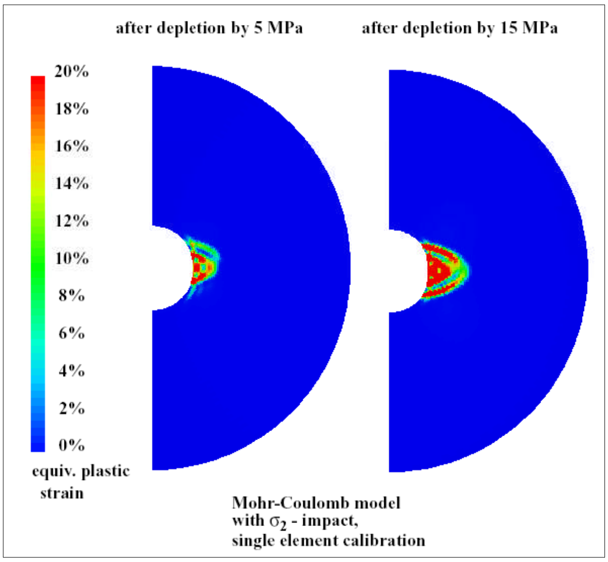

Figure 13 Openhole stability simulation using *Modified Mohr-Coulomb* criterion (with σ_2 impact). The numerical model is calibrated using a *single element* back-analysis of a polyaxial test. Results show plastic strain magnitude & localization around the hole wall with increasing depletion: 5 MPa (50 Bar), *left* & 15 MPa (150 Bar) *right*.

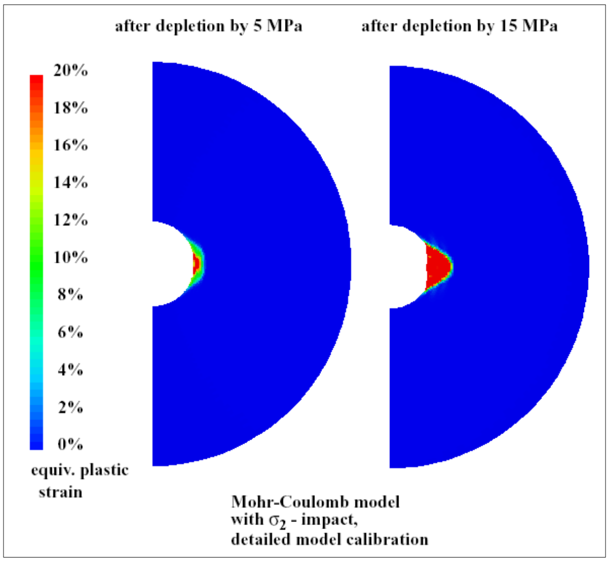

Figure 14 Openhole stability simulation using *Modified Mohr-Coulomb* criterion (with σ_2 impact). The numerical model is calibrated using a *finite element grid-based* back-analysis of a polyaxial test. Results show plastic strain magnitude & localization around the hole wall with increasing depletion: 5 MPa (50 Bar), *left* & 15 MPa (150 Bar) *right*.

6. ACKNOWLEDGEMENTS

The authors would like to acknowledge Norsk Hydro Oil & Gas for generously supporting the R&D work presented here and permitting its publication.

7. REFERENCES

1. Plischke, B., Kågeson-Loe, N, and Havmøller, O. 2004. Analysis of MLW open hole junction stability. Submitted to *Gulf Rocks 2004*.
2. Fjær, E and Ruistuen, H. 2002. Impact of the intermediate stress on the strength of heterogeneous rock. *J. Geophys. Res.* 107: 10,683–16,697.
3. Chang, C. and Haimson B. 2000. True triaxial strength and deformability of the German Continental Deep Drilling Program (KTB) deep hole amphibolite, *J. Geophys. Res*., 105, 18,999-19,013.
4. Ewy, R.T. 1998. Wellbore stability predictions using a modified Lade criterion. *Rock Mechanics in Petroleum Engineering*, v.1, pp 247-254. SPE.
5. Haimson, B. and Chang, C. 2000. A new true triaxial cell for testing mechanical properties of rock and its use to determine rock strength and deformability of Westerly granite. *Int. J. Rock Mech. Min. Sci*., 37, 285-296.
6. Handin, H., Heard, H.C. and Magouirk J.N. 1967. Effects of the intermediate principal stress on the failure of limestone, dolomite and glass at different temperatures and strain rates. *J. Geophys. Res*., 72, 611-640.
7. Kim, M.K. and Lade P.V. 1984. Modelling rock strength in three dimensions. *Int. J. Rock Mech. Min. Sci Geomech.Abstr*..,21, 21,-33.
8. Takahashi, M. and Koide, H. 1989. Effect of intermediate principal stress on strength and deformation behaviour of sedimentary rocks att eh depth shallower than 2000m. *Proc. Rock at Great Depth*, ed. V.Maury, pp.19-26. A.A.Balkema, Brookfield, Vt.
9. Wiebols, G.A. and Cook, N.G.W. 1968. An energy criterion for the strength of rock in polyaxial compression. *Int. J. Rock Mech. Min. Sci.*, 5, 529-549.
10. Sulem J, Vardoulakis I (1990). Bifurcation analysis of the triaxial test on rock specimens. *Acta Mechanica* 83, 195-212.
11. Mühlhaus, H.B., Vardoulakis,I 1987.: The thickness of shear bands in granular materials. *Geotechnique* 37, 271 -283